ADAPTIVE SMOOTHED PARTICLE HYDRODYNAMICS WITH APPLICATION TO GALAXY AND LARGE-SCALE STRUCTURE FORMATION [1]

Hugo Martel,[2] Paul R. Shapiro,[2]

Jens V. Villumsen,[3] and Hyesung Kang.[4]

University of Texas
McDONALD OBSERVATORY
PREPRINT No. 256

[1] To appear in *Smooth Particle Hydrodynamics in Astrophysics*, eds. G. Bono and J. Miller, *Memorie Della Societá Astronomica Italiana*, in press (1994)

[2] Department of Astronomy, University of Texas, Austin, TX 78712, USA.

[3] Department of Astronomy, Ohio State University, Columbus, OH 43210, USA.

[4] Department of Earth Sciences, Pusan National University, Pusan, 609-735 Korea.

ADAPTIVE SMOOTHED PARTICLE HYDRODYNAMICS WITH APPLICATION TO GALAXY AND LARGE-SCALE STRUCTURE FORMATION

HUGO MARTEL[1], PAUL R. SHAPIRO[1], JENS V. VILLUMSEN[2], HYESUNG KANG[3]
[1] *Department of Astronomy, University of Texas, Austin, TX 78712, U.S.A.*
[2] *Department of Astronomy, Ohio State University, Columbus, OH 43210 U.S.A.*
[3] *Department of Earth Sciences, Pusan National University, Pusan, 609-735 Korea.*

ABSTRACT. We describe a new version of the Smoothed Particle Hydrodynamics (SPH) method, called Adaptive Smoothed Particle Hydrodynamics (ASPH). The ASPH method is characterized by: (1) an anisotropic tensor smoothing length $\mathbf{H}$ and smoothing kernel which replace the standard scalar smoothing length h and isotropic kernel, and (2) the use of $\mathbf{H}$ to track shocks by predicting caustics, and thence to suppress spurious heating by artificial viscosity away from shocks. The resulting algorithm performs significantly better than the standard SPH method in situations involving highly anisotropic volume changes and strong shocks, which are common in cosmological simulations where the growth of density fluctuations leads to anisotropic gravitational collapse and supersonic infall. As a test, we have reproduced the cosmological pancake collapse solution over 4, 8, and 10 orders of magnitude in length, temperature, and pressure, with only ~ 30 particles per dimension per pancake. As further illustration, we apply ASPH in 2D to simulate structure formation in a Hot Dark Matter Universe.

1. Introduction

Most theories of galaxy formation assume that structure formed when initially small amplitude primordial density fluctuations grew by gravitational instability to nonlinear amplitude. Such primordial density fluctuations and gravitational instability lead to gravitational collapse, strong shocks, and radiative cooling, occurring over an enormous range of mass and length scales. Shocks, in fact, are the principal mechanism by which gravitational motions are dissipated so as to make formation of bound, star forming objects possible.

Motivated by this problem, we have developed a new version of the SPH method, called *Adaptive* SPH (ASPH), with substantially improved numerical resolving power and treatment of shocks compared to the original method (Shapiro *et al* 1994). Standard SPH (cf. Monaghan 1992 and references therein) suffers from two limitations which are particularly acute in simulations of cosmological structure formation by gravitational growth of density fluctuations, as follows: (1) the smoothing is isotropic, while gravitational collapse leads to highly anisotropic volume changes, and (2) supersonic collapse leads to strong shocks, requiring that artificial viscosity be introduced, but this results in widespread, spurious viscous heating of gas far from the shocks. ASPH solves these problems by: (1) introducing an anisotropic smoothing tensor and kernel which adjust

dynamically to follow anisotropic volume changes and vorticity, and (2) using this to track shocks by predicting the occurrence of caustics, and, thereby, to limit artificial viscous heating to those particles actually encountering a shock. In what follows, we describe our new version of SPH and show how and why it greatly enhances the dynamic range and resolving power of SPH to levels which promise to resolve the shocks which are generic to flows which form galaxies and large-scale structure.

2. Standard SPH

2.1. Isotropic Smoothing

SPH is a Lagrangian numerical hydrodynamics method which represents the fluid by a set of discrete gas "particles" which carry mass and thermal energy and move with the local flow velocity. These particles are essentially moving centers of interpolation for discretely representing the continuous flow variables and their variation in space. In standard SPH, the underlying continuous variation of each dependent variable $f(\mathbf{r})$ with position $\mathbf{r}$ is replaced by a spatially filtered, or smoothed, field $\tilde{f}(\mathbf{r})$,

$$\tilde{f}(\mathbf{r}) = \int f(\mathbf{r}) W(\mathbf{r} - \mathbf{r}', h) d^3\mathbf{r}' , \tag{1}$$

where W is a smoothing kernel function whose width is defined by the *smoothing length* h. For a *Gaussian kernel* in 3D, for example,

$$W(\mathbf{r} - \mathbf{r}', h) = \frac{e^{-|\mathbf{r}-\mathbf{r}'|^2/h^2}}{\pi^{3/2} h^3} . \tag{2}$$

In practice, $f(\mathbf{r})$ is actually known only at a finite set of irregularly spaced data points – the particle positions – so the integral is replaced by a finite sum over the particles.

The resolving power of SPH is, therefore, related to the smoothing length h, which defines the "zone of influence" of each particle. It is critical to adjust h for each particle so that it is comparable to the mean interparticle spacing Δx in the vicinity of that particle. If $h \ll \Delta x$, particles lose contact and the method breaks down. If, instead, $h \gg \Delta x$, SPH cannot resolve the underlying structure of the flow on the scale Δx.

Current versions of SPH adjust h both in time and space according to

$$h(\mathbf{r}, t) \propto \rho(\mathbf{r}, t)^{-1/D} , \tag{3}$$

where $\rho(\mathbf{r}, t)$ is the density and D is the dimensionality of the calculation (i.e. $D = 1, 2,$ or 3 for 1D, 2D, or 3D, respectively, in Cartesian coordinates). This is intended to make $h \sim \Delta x(\mathbf{r}, t)$, the local interparticle spacing, everywhere at all times. This is strictly valid only for *isotropic* volume changes, however. The spacing Δx at a given location at a given time can vary in *direction*, as a result of anisotropic contraction or expansion. Equation (3) only ensures that the smoothing length of any given particle will be of the order the mean distance to its neighbors, *averaged* over *all* directions. In anisotropic compression, however, this h does not shrink fast enough in the direction of maximum contraction, leading to a loss of resolution, while in the direction transverse to this contraction, h

shrinks even if there is *no* contraction in this direction, and particles can eventually lose contact. Anisotropic contraction or expansion is very common in astrophysical problems, especially those involving gravitational collapse and strong shocks, so it is desirable to developed a version of SPH which is not limited to this isotropic smoothing approach.

2.2. Artificial Viscosity

Artificial viscosity must be introduced in the SPH equations for momentum and energy conservation in order to handle shocks and prevent particle interpenetration, or trajectory crossing. Supersonic compression such as that generic to gravitational collapse on scales $\lambda > \lambda_J$ (the Jeans length), which occurs commonly in galaxy and large-scale structure formation, then leads to widespread, spurious viscous *heating* of gas far from the shock. This "preheating" can be particularly devastating in flows involving radiative cooling. It is desirable, therefore, to find a way to restrict the effects of artificial viscosity in SPH to the actual shock transition.

3. The Adaptive Smoothed Particle Hydrodynamics (ASPH) Method

3.1. Anisotropic Smoothing

We have developed a new version of SPH, called Adaptive SPH, which is designed to handle situations involving anisotropic volume changes. We introduce the concept of *anisotropic smoothing tensor* H, a smoothing length which varies with time, space, *and direction*. In this new formalism, the spherical zone of influence of a given particle is replaced by a triaxial ellipsoid. Each ellipsoid is defined by a triad of mutually perpendicular vectors, the semimajor axes of the ellipsoid, which have three components each. We refer to this ensemble of nine components as the *H-tensor* of the particle. The length of each semimajor axis is determined by the local interparticle spacing along the direction of that axis. The H-tensors are dynamically evolved by the ASPH code using the components of the deformation tensor $\partial v_i/\partial x_j$ to follow the local deformation and vorticity of the flow. For flows with no vorticity, the H-tensor triad of axes $\mathbf{h}_k$ are just the principal axes of the deformation tensor, with lengths that change in a time δt in proportion to $(1 + \lambda_k \delta t)$, where the λ_k's are the eigenvalues of $\partial v_i/\partial x_j$ and the $\mathbf{h}_k$'s point along the eigenvectors. With vorticity, the axes $\mathbf{h}_k$ must rotate to take account of the anti-symmetric part of $\partial v_i/\partial x_j$. In ASPH, the 3D Gaussian kernel of particle i and position $\mathbf{r}_i$, evaluated at position $\mathbf{r}_j$, is given by

$$W_3(\mathbf{r}_{ij}, \mathbf{H}) = W_1(x', h_1) W_1(y', h_2) W_1(z', h_3) = \left[\frac{e^{-x'^2/h_1^2}}{\pi^{1/2} h_1}\right]\left[\frac{e^{-y'^2/h_2^2}}{\pi^{1/2} h_2}\right]\left[\frac{e^{-z'^2/h_3^2}}{\pi^{1/2} h_3}\right], \quad (4)$$

where $\mathbf{r}_{ij} = \mathbf{r}_i - \mathbf{r}_j$, W_1 and W_3 are the 1D and 3D Gaussian kernels, respectively, $h_1 = |\mathbf{h}_1|$, $h_2 = |\mathbf{h}_2|$, $h_3 = |\mathbf{h}_3|$ are the semimajor axes of the ellipsoid, and x', y', and z' are the projections of $\mathbf{r}_{ij}$ along each of these axes.

This technique has three strong advantages over standard SPH: (1) The resolving power of the SPH equations in regions with strong anisotropy can be increased by orders of magnitude. (2) The H-tensors track the Lagrangian deformation of the flow, and consequently each particle keeps roughly the same set of neighbors for many timesteps. This

implies that the usually costly nearest-neighbor search need be done only occasionally instead of at every timestep, resulting in a large speed-up of the algorithm. (3) Caustics and shocks in the flow can be predicted to occur whenever a particle's H-tensor ellipsoid shrinks along one or more of its axes enough to make the volume go to zero. This forms the basis for our shock-tracking algorithm below.

3.2. Shock tracking and Artificial Viscosity

The evolving H-tensors track the local deformation of the fluid. Without artificial viscosity, particle crossing would occur whenever a particle encounters a shock, and this would result in an "inversion" of the H-tensor for this particle, with the shortest axis shrinking to negative values. The ASPH method makes use of this phenomenon by turning artificial viscosity on in the energy equation *only* for particles whose H-tensor is about to undergo this inversion. This automatically restricts artificial viscous heating to just those fluid particles which are actually encountering a shock.

4. Testing the Anisotropic H-Tensor and Smoothing: 1D and 2D Kinematic Flows

We call ***kinematic flow*** a flow in which we impose trajectories on fluid particles, according to some prescribed velocity field which satisfies the continuity equation. Thus, we do not compute the forces on the particles, or if we do, then we do not use these forces to advance the particle velocities. Such flows are particularly useful for testing the calculation of smoothed quantities, or the evolution of the H-tensor, since inaccuracies in these calculations do not feed back on the particle motions.

4.1. 1D Flow: Plane Wave Density Perturbation

Consider the growing mode of a 1-D, sinusoidal, adiabatic, plane wave, cosmological density fluctuation of comoving wavelength λ_p in an Einstein-de Sitter universe. The perturbed comoving position x of the mass element whose unperturbed position is q is

$$x = q - \frac{\delta(t_i)}{2\pi} \sin \frac{2\pi q}{\lambda_p} \tag{5}$$

at initial time $t = t_i$ at which the amplitude $\delta(t_i) \ll 1$. The initial density is given by

$$\rho = \frac{\bar{\rho}(t_i)}{1 - \delta(t_i) \cos 2\pi q/\lambda_p}, \tag{6}$$

and initial velocity is given by

$$v_x = -\frac{H_0}{2\pi} \left(\frac{a_i}{a_0}\right)^{-3/2} \delta(t_i) \sin \frac{2\pi q}{\lambda_p}, \tag{7}$$

where a is the scale factor, $a_i = a(t_i)$, $a_0 = a_{\text{present}} = 1$, H_0 is the Hubble constant, and $\bar{\rho}(t_i)$ is the mean density at t_i.

Exact Nonlinear Solution. In units with $\lambda_p = 1$, the unperturbed position ranges from $q = -1/2$ to $q = +1/2$, with a density singularity, or caustic, forming at $x = q = 0$ at time t_c and scale factor a_c. The perturbation amplitude grows as $\delta(t) = \delta(t_i)a(t)/a_i = a(t)/a_c$. We chose $a_i = 1/28$ and $a_c/a_i = 4$. The perturbed position, density, and peculiar velocity are then given for all $t < t_c$ and $a < a_c$ by equations (5)–(7) with $\delta(t_i)$ and a_i replaced by $\delta(t)$ and $a(t)$, respectively. This solution is exact up to the moment of caustic formation even when $\delta \gg 1$. Since the flow is adiabatic for $t < t_c$, the pressure and pressure-force acceleration are given by

$$P(t)/\bar{P}(t_i) = \left[\rho(t)/\bar{\rho}(t_i)\right]^{\gamma}, \tag{8}$$

and

$$F_p = -\frac{1}{\rho}\frac{\partial P}{\partial x} = 2\pi\gamma\delta[\bar{P}(t_i)/\bar{\rho}(t_i)](\sin 2\pi q)(1 - \delta\cos 2\pi q)^{-(\gamma+1)}, \tag{9}$$

where $\gamma = 5/3$ and where $\bar{P}(t_i)$ is the mean pressure at $t = t_i$.

The Test: 60 particles in the range $-1/2 \leq q \leq 1/2$ are moved with time along trajectories given by equation (5), with velocities given by equation (7) [with $\delta(t)$ and $a(t)$ replacing $\delta(t_i)$ and a_i]. The exact solution above also yields the values of ρ, P, and $\partial v_x/\partial x$ at each particle location at all times. The *smoothed* values of ρ and F_p are then calculated using the smoothing algorithms of ASPH and SPH, respectively, with these exact values for x, v_x, ρ, P, and $\partial v_x/\partial x$ for each particle. For ASPH, the H-tensors are evolved using $\partial v_x/\partial x$ (so $h_x \propto \rho_{exact}^{-1}$ in the collapse direction), while for SPH, $h \propto \rho_{exact}^{-1/3}$ is assumed. The smoothed ρ and F_p are shown along with the analytical solutions in Figure 1 for $a/a_c = 0.975$. The ASPH results for both ρ and F_p are in excellent agreement with the exact results and are much more accurate than those of SPH in the central region where nonlinear amplitude and gradients are large. The smoothing length h of standard SPH did not shrink fast enough to follow the anisotropic collapse of the system, causing oversmoothing of the central region ($h \gg \Delta x$), which results in a serious underestimate of both ρ and F_p.

4.2. 2D Flow: Deformation and Vorticity

In order to test the method in the presence of vorticity, we consider a purely kinematical 2D flow given by $v_x = c_1 y + c_2 x^2/2$, $v_y = c_3 x$. For such a flow, $\nabla \cdot \mathbf{v} = c_2 x$ and $\nabla \times \mathbf{v} = c_1 - c_3$. As long as $c_1 \neq c_3$, this flow is rotational (i.e. has vorticity). We take $c_1 = 1$, $c_2 = 0.5$, $c_3 = 3$, with uniform density at time $t = 0$.

For any fluid element at initial position $\mathbf{x}_0$ at time $t = 0$, we can solve the above equations for $\mathbf{x}(\mathbf{x}_0, t)$ and $\partial v_i/\partial x_j(\mathbf{x}_0, t)$ by the Runge-Kutta method to arbitrarily high accuracy. We use this $\mathbf{x}(\mathbf{x}_0, t)$ to track the motion of a set of particles at initial $\mathbf{x}_0$'s corresponding to a square lattice grid of spacing Δx, integrate the continuity equation to solve for densities $\rho(\mathbf{x}_0, t)$, and use $\partial v_i/\partial x_j(\mathbf{x}_0, t)$ to evolve the H-tensors for these particles. For standard SPH, the smoothing length h is taken to vary as $\rho^{-1/2}$. The results are shown on Figure 2, where we focussed on the particle located initially and at all times at $x = y = 0$, for which $\rho =$ constant. The circles and ellipses represent the zones of influence of that particle for standard SPH and ASPH, respectively. We mark

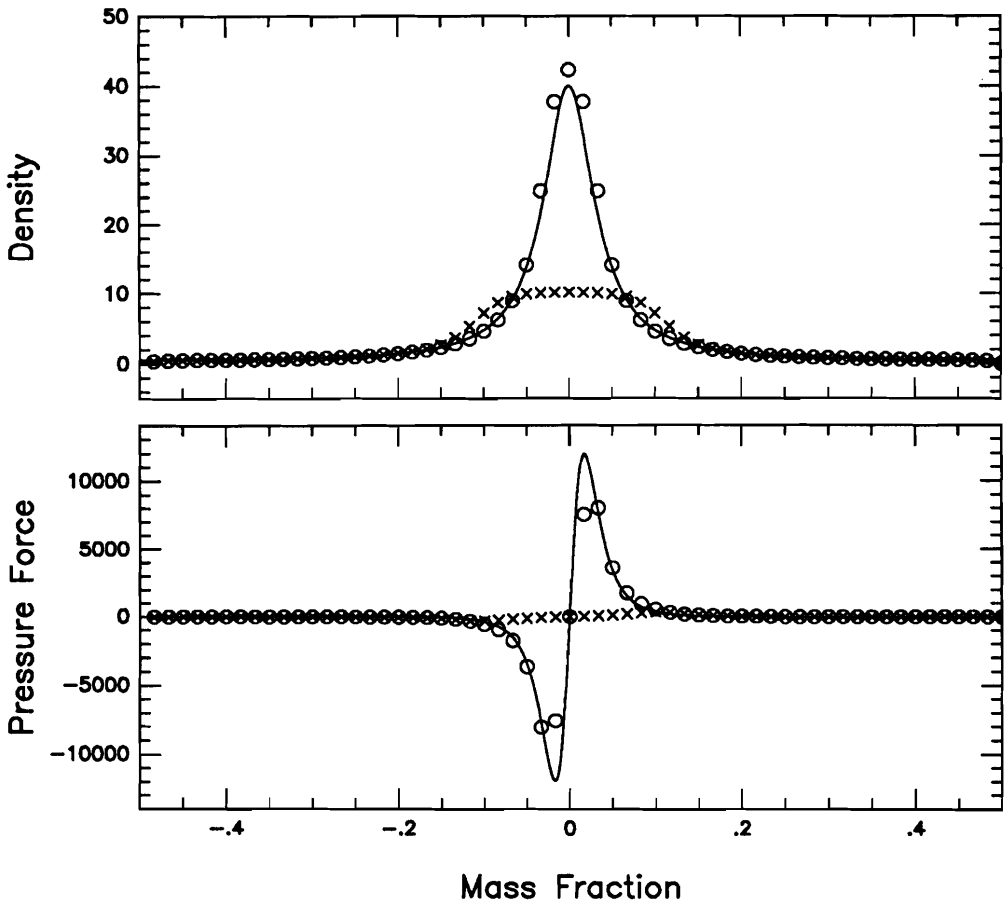

Fig. 1. ρ and F_p versus q for 1D Plane-Wave Perturbation at $a/a_c = 0.975$. ASPH (open circles), SPH (crosses), exact solution (line).

the particles which are initially the nearest neighbors of this central particle (boldface particles), all those particles within the circle of radius $3h = 6\Delta x$ at $t = 0$. For SPH, the circle remains unchanged in time, while for ASPH the circle becomes the ellipse with axes defined by the component axes $\mathbf{h}_k$ of the tensor $\mathbf{H}$. Figure 2 shows how well the anisotropic smoothing ellipse of ASPH stretches and rotates so as to track the motion of these neighbors, while the SPH circle defined by isotropic h fails badly.

5. The Cosmological Pancake Collapse Test Problem

A difficult, fully dynamical test which all methods which are to be applied to cosmological flows should be required to pass is that of the gravitational collapse of a 1D, plane wave

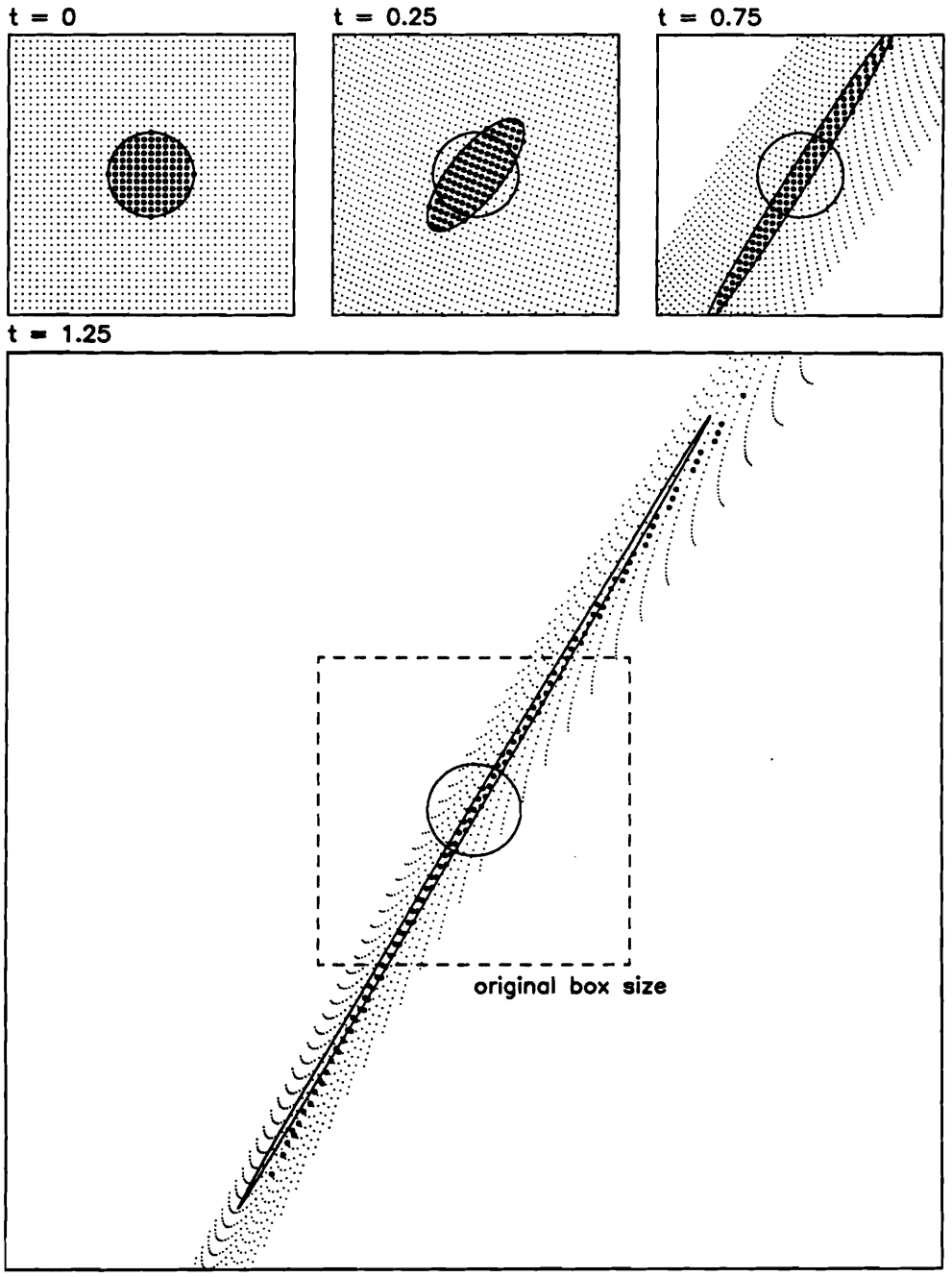

Fig. 2. Particle Positions (dots) for 2D Kinematic Flow with Vorticity at 4 time-slices as labelled.

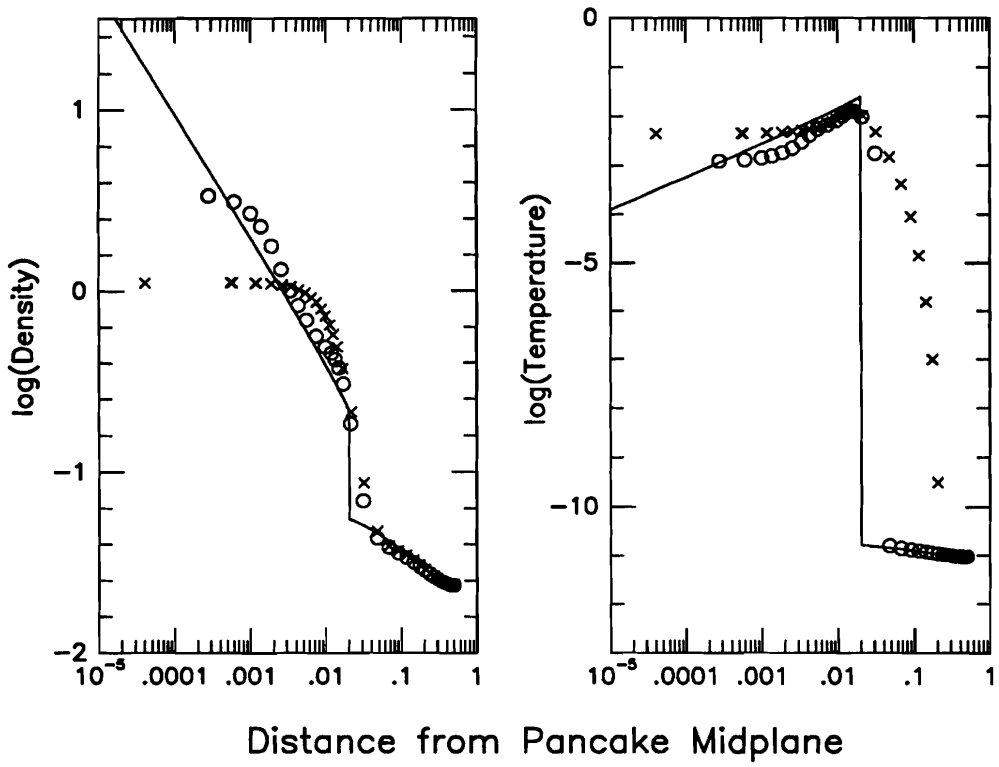

Fig. 3. 2D Tilted, Shifted Pancake test results at $a/a_c = 1.5$. ASPH (open circles), SPH (crosses), and exact solution (solid line). Dimensionless computational units.

density fluctuation in a universe comprised of baryons and collisionless dark matter. This is the cosmological pancake problem, in which an initially linear amplitude density fluctuation grows to nonlinear amplitude, forms a caustic in the dark matter distribution located in the plane of symmetry of the pancake and strong accretion shocks, one on each side of this central plane, followed by continued infall, phase-mixing of the dark matter, and radiative cooling of the shocked baryon-electron plasma. Detailed, 1D numerical solutions for this problem already exist (Shapiro, Struck-Marcell, and Melott 1983; Bond *et al* 1984; Shapiro and Struck-Marcell 1985), as do approximate analytical solutions (Struck-Marcell, Shapiro, and Martel 1994), for comparison.

The initial condition prior to caustic and shock formation is the same as for the 1D kinematic test discussed in § 4.1. We evolve the system from initial scale factor $a_i = 1/28$ (redshift $z = 27$) thru the epoch of shock and caustic formation at $a_c/a_i = 4$ ($z = 6$) to $a_f/a_i = 6$ ($z = 3.6667$). Radiative cooling is neglected. Our ASPH method, in principle, can automatically identify and adjust to accommodate a pancake collapse and

shocks along *any* direction, not known *a priori*. Testing this fully requires at least a 2D calculation (i.e. in this case (x,y) Cartesian coordinates). We therefore use a 2D version of the SPH and ASPH methods, respectively, and solve the gravitational force problem by using a standard Particle-Mesh (PM) method. For 2D SPH, the smoothing length $h \propto \rho^{-1/2}$. The computational volume is a square box with periodic boundary conditions and one edge-on pancake of wavelength $\lambda_p = L_{box}/\sqrt{2}$, oriented with its symmetry plane (*i.e.* density maximum) at 45° with respect to the walls of the computational box, shifted away from the box center. We take $N_{gas} = N_{DM} = 64 \times 64 = 4096$ equal-mass particles of each type (dark matter and gas) with initial positions displaced by the perturbation away from the same square uniform lattice. This is designed to test that ASPH can adjust to follow the anisotropic collapse of the pancake regardless of its orientation. (*NOTE:* Given the 45° tilt, there are now only 22 gas particles per row perpendicular to the pancake plane to resolve the flow on each side of the central plane.) The PM calculation uses a square lattice grid with $128 \times 128 = 16,384$ cells.

Figure 3 shows a comparison of the SPH and ASPH results plotted against the analytical solution (Struck-Marcell, Shapiro, and Martel 1994) at $a_f/a_c = 1.5$, after shock and caustic formation. The ASPH solution matches the analytical solution over 4 orders of magnitude in length with only 22 particles! ASPH resolves the postshock temperature profile and achieves the required jump of 8 orders of magnitude in temperature across the shock. Moreover, it generally does so with no more than one particle whose temperature is intermediate between the pre- and post-shock values, to spread the shock transition along the direction normal to the shock. Standard SPH, on the other hand, artificially heats a wide range of the preshock particles, spreading the shock transition out by a spurious factor of 10 in distance and failing to resolve properly the slope of the postshock temperature profile.

6. An Illustrative Example: 2D Simulation of a Hot Dark Matter Universe

We apply our ASPH method in 2D to simulate the growth of large-scale structure in a universe dominated by Hot Dark Matter, with initial density fluctuations given by Gaussian random noise based upon a Harrison-Zel'dovich primordial power spectrum ($n = 1$) with amplitude fixed by the COBE satellite detection of CMB anisotropy. The 2D power spectrum is the same as in 3D, but multiplied by $2k$ ($k = L_{box}/\lambda$, $\lambda =$ wavelength, $L_{box} =$ size of square computational box) — i.e. equal rms $\delta\rho/\rho$ for equal fluctuation scale length. We couple our ASPH method to a standard Particle Mesh (PM) gravity solver in 2D. We take $h = 0.5$, $\Omega = 1$, $\Omega_{DM} = 0.9375$, $\Omega_b = 0.0625$, $N_{particles} = 256 \times 256 = 65,536$ of which 1/16 are gas, so that $N_{gas} = 64 \times 64 = 4,096$, with initial positions perturbed away from a uniform square lattice in a simulation box of side $L_{box} = 200$ Mpc (present units) with 512×512 PM cells and periodic boundary conditions, at initial redshift $z_i = 24$. The initial density fluctuations are represented as the superposition of plane wave perturbations with random phases, including all wavevectors which satisfy periodic boundary conditions with dimensionless wavenumber k in the range $1 \leq k \leq 32$. Radiative cooling is neglected.

In Figure 4, we zoom in on a particular region of the computational box, a square of size 22 Mpc, containing an already-formed pancake, merging at an oblique angle with

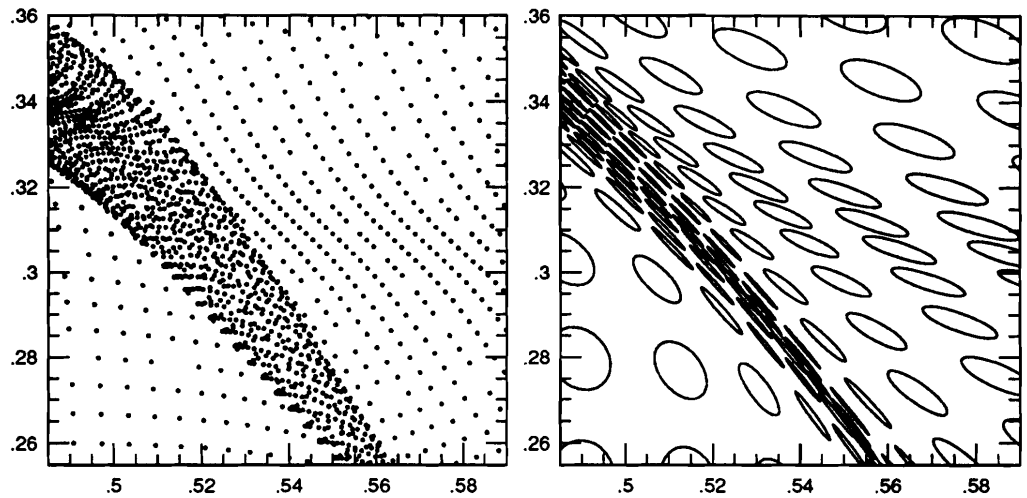

Fig. 4. Zoom in at $z = 0$. Dark matter (left panel), H-tensor ellipses (right panel).

an incipient (i.e. pre-emergent) pancake. The idea is to check whether the H-tensors of the ASPH code are "aware" of the directions and degrees of collapse of both pancakes. Figure 4a shows the dark matter particle positions in that particular subregion, with the two edge-on pancakes, one post- and one pre-caustic. Figure 4b shows the H-tensor ellipses for the gas particles, scaled by a factor 0.15 for clarity (otherwise they would overlap). The ASPH code successfully identified both the presence and degree of collapse of *both* pancakes, and has deformed and oriented the H-tensors accordingly.

Finally, we illustrate the problem which standard SPH has simulating flows like this, causing the widespread, spurious preheating of contracting regions of the flow far from shocks by artificial viscosity, and show the improvement which ASPH makes. Figure 5 shows the positions of all gas particles for the full computational box. We identify a subset of these as numerically "shocked particles" (that is, particles that have been shock-heated at some point during the simulation) if they are particles whose temperature significantly exceeds their "adiabatic temperature" defined by

$$T_{ad} = T_i(\rho/\rho_i)^\gamma \,, \tag{10}$$

where ρ_i and T_i are the particle's initial density and temperature. These are particles which have experienced artificial viscous heating. We have distinguished the subset of gas particles for which $T > 10T_{ad}$ from the rest of the gas particles by open circles (SPH results) and filled circles (ASPH results). In standard SPH, the viscous preheating is so

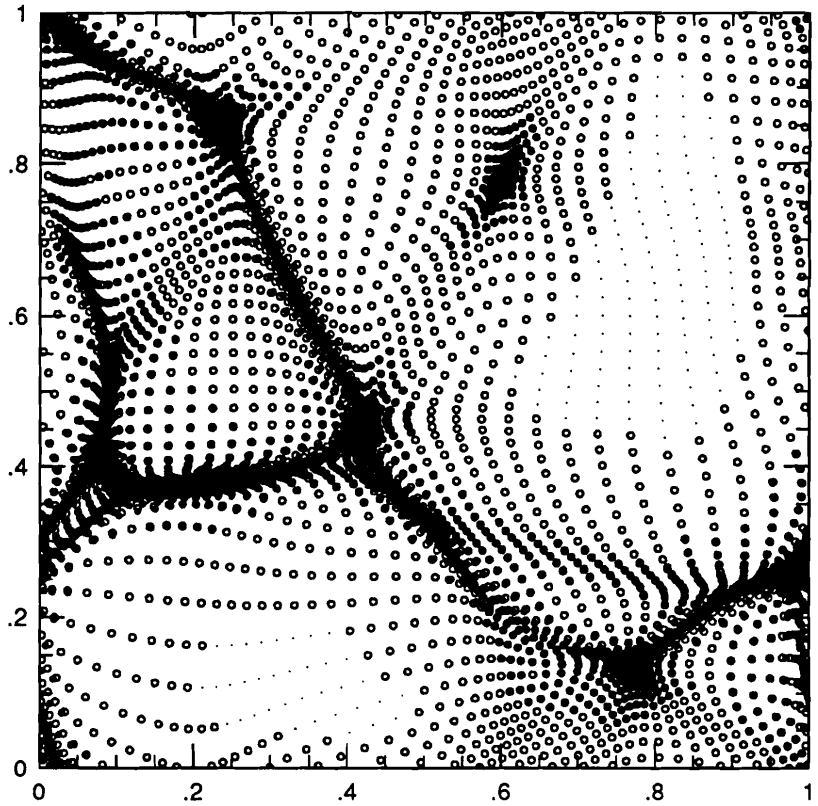

Fig. 5. Gas Particles at $z = 0$. Shock-heated: SPH (open circles), ASPH (filled circles).

severe that almost the entire system has been "shocked." The ASPH method, with its shock-tracking algorithm and its switch for controlling artificial viscous heating, does much better, limiting "shock-heating" to the pancakes and their intersections.

Acknowledgements

We are grateful for the support of NASA NAGW-2399, Robert A. Welch F-1115, the University of Texas System Center for High Performance Computing, the Ohio Supercomputer Center, and the NSF NCSA, and discussion with J. Monaghan and M. Owen.

References

Bond, J. R., Centrella, J., Szalay, A. S., and Wilson, J. R., 1984, *M.N.R.A.S.*, **210**, 515.
Monaghan, J. J., 1992, *Ann. Rev. Astron. Ap.*, **30**, 543.
Shapiro, P. R., and Struck-Marcell, C., 1985, *Ap. J. Suppl.*, **57**, 205.
Shapiro, P. R., Martel, H., Villumsen, J. V., and Kang, H., 1994, *Ap. J.*, to be submitted.
Shapiro, P. R., Struck-Marcell, C., and Melott, A. L., 1983, *Ap. J.*, **275**, 413.
Struck-Marcell, C., Shapiro, P. R., and Martel, H., 1994, in preparation.